

Describing Functions and Phase Response Curves of Excitable Systems

Robin Wroblowski¹, Rodolphe Sepulchre^{1,2}

Abstract—The **describing function (DF)** and **phase response curve (PRC)** are classical tools for the analysis of feedback oscillations and rhythmic behaviors, widely used across control engineering, biology, and neuroscience. These tools are known to have limitations in networks of relaxation oscillators and excitable systems. For this reason, the paper proposes a novel approach tailored to excitable systems. Our analysis focuses on the discrete-event operator mapping input trains of events to output trains of events. The methodology is illustrated on the excitability model of Hodgkin-Huxley. The proposed framework provides a basis for designing and analyzing central pattern generators in networks of excitable neurons, with direct relevance to neuromorphic control and neurophysiology.

I. INTRODUCTION

The system analysis of rhythmic activity in neuronal networks is a central problem both in neuroscience and in neuromorphic engineering. Traditionally, tools such as the describing function (DF) and phase response curve (PRC) have been instrumental for engineers and biologists in characterizing and predicting oscillatory behaviors [1], [2]. These methods provide insight into the feedback mechanisms of oscillators and into phase-locking phenomena. They guide much of our understanding of rhythm generation and synchronization.

The describing function method is inherited from harmonic balance analysis, which assumes quasi-harmonic oscillations. In contrast, neural oscillators are known to exhibit event behaviors characterized by switch-like transients and fast-slow dynamics [3]. Excitable systems do not oscillate on their own. Instead, they generate action potentials (spikes) in response to triggering stimuli [4]. Likewise, phase response curve methods rely on variational methods that assume smooth dynamics and weak coupling. As such, they are not directly applicable to excitable systems.

Motivated both by the appeal of those analysis methods and by the limitations they exhibit in neural networks, the present paper investigates how the concepts of describing function and phase response curve can be adapted to excitable systems. To that end, we regard an excitable system as an input-output discrete-event model mapping periodic sequences of input events (presynaptic voltage spikes) to output events (postsynaptic voltage spikes). The proposed

The research leading to these results has received funding from the European Research Council under the Advanced ERC Grant Agreement SpikyControl n.101054323.

Email: robin.wroblowski@kuleuven.be, rodolphe.sepulchre@kuleuven.be.

¹KU Leuven, Department of Electrical Engineering (ESAT), STADIUS Center for Dynamical Systems, Signal Processing and Data Analytics, Kasteelpark Arenberg 10, 3001 Leuven, Belgium.

²Department of Engineering, University of Cambridge, Trumpington Street, Cambridge CB2 1PZ, United Kingdom.

describing function computes the phase shift of those sequences as a function of the period. We define the event phase response curve in a similar fashion: starting from a nominal periodic discrete-event oscillation, we study the phase advance or phase delay caused by periodic impulsive perturbations as a function of their relative phase to the nominal oscillator.

Our analysis suggests that those adaptations of classical tools retain their simplicity and insight while showing strong predictive power in networks of excitable systems. They capture the important property that oscillations in networks of excitable nodes consist of ‘event sequences’ rather than ‘harmonics’.

The approach draws particular inspiration from recent work such as that by Huo *et al.* [5], who demonstrated spiking CPG design using winner-takes-all topologies and rebound excitable neurons.

By extending classical analysis tools, our framework aims to provide simple and practical methods to design and control rhythmic networks from excitable components, advancing the development of applications within the field of neuromorphic engineering.

II. MOTIVATION: BACKGROUND & LIMITATIONS

This section revisits two classical tools for the analysis of nonlinear oscillators: the describing function (DF) and the phase response curve (PRC). Both methods are highly effective when the oscillations are weakly nonlinear or quasi-harmonic. Instead, they face methodological difficulties and lack predictive power when the oscillations are of the relaxation-type. Recent work has proposed various strategies to address these limitations, yet unlike such oscillator-based extensions, our approach departs from the harmonic assumptions in favor of an event-based framework suited to excitable systems.

A. Describing functions

The describing function method was originally developed for the feedback interconnection of a linear time-invariant system with a static nonlinearity. The describing function $N(A, \omega)$ of the static nonlinearity expresses the gain and phase shift introduced by the nonlinear element when driven by a sinusoidal input of amplitude A and frequency ω :

$$N(A, \omega) = G(A, \omega) e^{j\varphi(A, \omega)}, \quad (1)$$

where $G(A, \omega)$ is the amplitude gain and $\varphi(A, \omega)$ the corresponding phase shift. For dynamic nonlinearities, both quantities depend on input amplitude and frequency [6].

The DF method is a special case of the more general method of harmonic balance, approximating nonlinear periodic solutions using only the fundamental harmonic component. By modeling the nonlinearity as a complex gain, the method captures how amplitude and phase of a single harmonic signal are modified when neglecting the higher harmonics. This approximation is reliable only when the system has strong low-pass characteristics, ensuring that higher harmonics are attenuated [7].

Despite its simplifying assumptions, the DF method has proven very useful to predict the existence and stability of oscillations in nonlinear systems. However, in relaxation oscillators or slow-fast systems, such as biological neurons, square-wave oscillations and abrupt nonlinear transitions violate its assumptions, leading to inaccuracies [8], [6]. In these cases, DFs capture only qualitative oscillatory behavior, motivating alternative formulations for non-harmonic or discrete-event dynamics.

B. Phase response curves

The phase response curve (PRC) quantifies how a small perturbation applied to a nominal oscillation affects the phase of the steady-state behavior. It describes the phase sensitivity of an oscillator and supports analysis of synchronization and entrainment [2], [4], [9], [10].

Classical phase reduction theory simplifies high-dimensional oscillator dynamics to a single scalar phase, assuming rapid amplitude relaxation, weak coupling, and sufficient timescale separation [9]. Within this framework, the infinitesimal PRC (iPRC) corresponds to the gradient of the asymptotic phase function and measures instantaneous phase sensitivity [1]. Under weak stimulation, finite perturbations can be approximated via convolution of the iPRC with the input waveform.

Analytical expressions for the iPRC exist for simple systems, but for high-dimensional or strongly nonlinear oscillators they must be computed numerically. PRC-based analysis degrades in systems with pronounced timescale separations or discontinuities, where switch-like trajectories violate smoothness assumptions [11].

PRCs also provide a direct means to analyze and predict phase locking. Zero crossings of the PRC indicate potential locked states, and the slope at those points determines their stability. When oscillator and input frequencies are nearly equal, reduced models such as the Adler or Kuramoto equations adequately describe synchronization; otherwise, a more general integral formulation is required [12].

Beyond descriptive use, PRCs support control design strategies for oscillator synchronization and phase stabilization [13], [14].

C. Limitations

Both methods rely on the assumption of steady-state endogenous oscillations and harmonic balance. Those assumptions are at odds with the nature of excitable neurons: excitable neurons do not oscillate endogenously. Instead, they produce spiking events in response to triggering stimuli.

Moreover, the nature of the event is strongly localized in time, in sharp contrast to the harmonic oscillations that are strongly localised in frequency. Describing functions overlook non-harmonic dynamics and cannot represent systems that respond through discrete events rather than continuous motion. Similarly, PRCs assume a stable limit cycle and small perturbations of the limit cycle, in contrast to the forced nature of event oscillations [9].

Extensions of PRC theory have attempted to relax these constraints. Izhikevich [15] reformulated phase response theory for relaxation oscillators, and Sacré and Franci [11] proposed the singular PRC for the limit of strong timescale separation.

Two notable extensions for excitable or transiently active systems are the functional PRC (fPRC) and the isostable response curve (IRC). The fPRC [16], [17] measures phase shifts relative to discrete trajectory events under periodic stimuli, offering a way to capture adaptive timing in non-oscillatory neurons. However, it typically requires stimulus inputs generated online from previous events and employs fixed pulse shapes rather than synaptically filtered events. The IRC approach [18] instead builds on isostables (surfaces of equal return rate to equilibrium) to characterize excitable dynamics near rest.

Despite these advances, none of the existing methods adequately capture the input-output behavior or sensitivity of excitable mechanisms such as post-inhibitory rebound, which lack intrinsic periodicity and cannot be parameterized by a continuous phase. These limitations motivate a new framework grounded in discrete, excitable events rather than continuous oscillations.

III. DISCRETE-EVENT MODELING OF EXCITABLE SYSTEMS

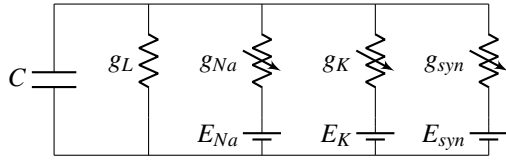
Given the limitations of oscillator-based methods, we focus on the fundamentally event-driven nature of biological neuronal networks, where discrete voltage spikes trigger synaptic currents that propagate through chains of excitable events rather than continuous oscillations. Since Hodgkin and Huxley [19], neuronal excitability has been modeled by conductance-based circuits (Figure 1a), while simplified models such as integrate-and-fire, FitzHugh-Nagumo, and rate-based models provide computationally and analytically tractable abstractions [20].

The membrane voltage V in conductance-based models follows the RC-circuit equation:

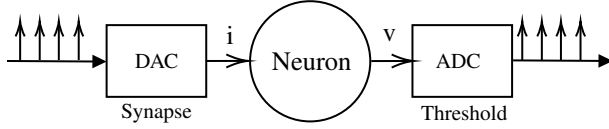
$$C \frac{dV}{dt} = \sum_k I_k, \quad I_k = g_k(t)(V - E_k),$$

where C is the membrane capacitance, $g_k(t)$ are voltage-dependent conductances, and E_k the reversal potentials.

Figure 1a shows the electrical circuit model of an excitable neuron joined by a synapse, receiving presynaptic voltage as input and producing membrane voltage as output. Internal currents depend on the neuron voltage, while synaptic currents depend on presynaptic voltage.



(a) Circuit Diagram of the excitable neuron model



(b) Input-output diagram representation of the discrete-event node. The synapse maps events to currents (DAC), the neuron maps currents to voltages and the threshold maps the voltages into events (ADC).

Fig. 1: Excitable neuronal circuit and discrete-event model of fundamental excitable node.

For the remainder of the paper, the internal currents correspond to Hodgkin-Huxley channels (I_L , I_{Na} , I_K), while we adopt a generic synaptic conductance model:

$$g_{syn}(t) = \bar{g}_{syn} h, \quad (2)$$

$$\dot{h} = \frac{\alpha(1-h)}{1 + \exp\left(\frac{-(V_{pre}-V_{th})}{k}\right)} - \beta h, \quad (3)$$

where \bar{g}_{syn} is the maximal conductance, $\beta = \tau_{decay}^{-1}$, $\alpha = \tau_{rise}^{-1} - \beta$, V_{th} the half-activation constant, and k the sigmoid slope.

These excitable systems serve as nodes forming an event-based network, interacting exclusively through discrete events. The discrete-event node shown in Figure 1b is central to our experiments.

The excitable circuit defines a continuous-time mapping from presynaptic voltage spikes to postsynaptic spikes. Importantly, this framework is not limited to Hodgkin-Huxley neurons or specific synapse models. The only requirements are: (1) an event-to-current mapping (discrete-to-analog conversion, DAC) for the synapse, and (2) a current-to-event mapping (analog-to-discrete conversion, ADC) for the neuron.

To associate a discrete-event model with a continuous-time excitable system, spikes are abstracted as Dirac impulses $\delta(t - t_i)$. This models neuronal communication as a mapping from event sequences to event sequences, consistent with biological spikes triggering synaptic currents. The proposed representation exclusively considers models in the 1:1 phase-locking mode, in which each input event triggers exactly one output event, creating a one-to-one mapping between event sequences.

IV. EVENT DESCRIBING FUNCTIONS

The discrete-event modeling framework introduced in Section III captures the fundamental event-driven nature of excitable neuronal systems, where spike events, rather than continuous oscillations, govern system dynamics. Within this perspective, we develop an analogous description to the

classical describing function method, but tailored for event-based input-output signals. This leads to the concept of the *event describing function* (eDF), which characterizes the phase relationship between sequences of input and output events of an excitable system.

Since the input and output signals consist of unitary events, the eDF focuses solely on phase differences. When the input event sequence has a sufficiently large period $T > T_{\min}$, output events become phase-locked, or *entrained*, to the input in steady state. This steady-state behavior enables us to define the eDF as the event delay $\Delta(T)$ divided by the input period T , yielding a relative phase shift:

$$\varphi(T) = \frac{\Delta(T)}{T}. \quad (4)$$

This exclusive focus on timing relationships is justified by biologically grounded assumptions that disregard gain and amplitude dependence. Throughout this paper, timing is expressed via the period $T = \frac{2\pi}{\omega}$, consistent with conventional neuroscience notation.

A. Case study: eDF of a Hodgkin-Huxley neuron

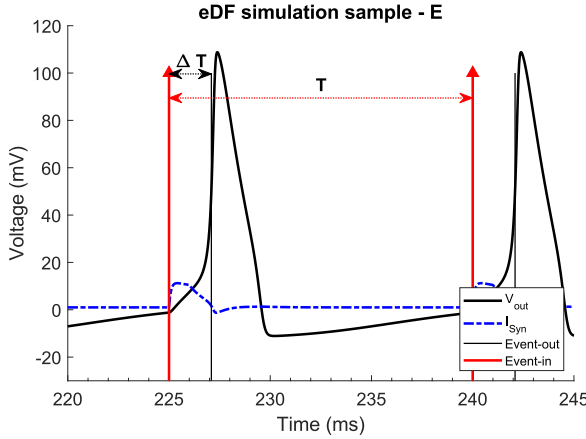
This section analyzes the event describing function as a tool to characterize the input-output behavior of the fundamental excitable node within the discrete-event modeling framework. The steady-state relative phase shift $\varphi(T)$ between the event signals is obtained through numerical integration, from which the eDF is constructed by simulating across a range of input signal periods.

Figure 2 presents two examples of eDF simulations for an inhibitory node with period $T = 25$ and an excitatory node with $T = 15$ at steady state. The plots display input events (red vertical arrows), synaptic current (blue), output voltage (black), and output events (black vertical lines). Notably, the rebound spike onset is significantly larger, as it occurs only after inhibition is released.

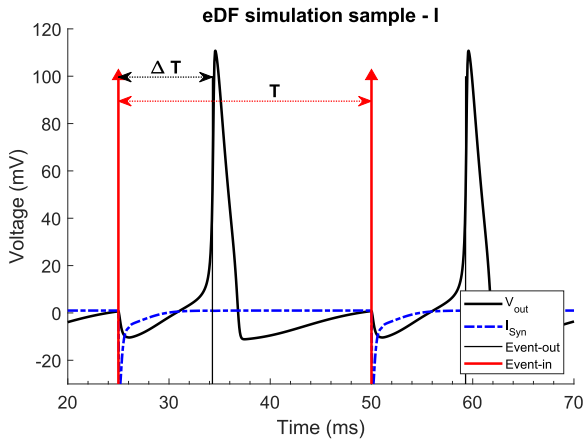
Figure 3 compares the eDF curves of a Hodgkin-Huxley neuron receiving inhibitory or excitatory synaptic input. The upper panel shows absolute event onset times over a range of input periods. As expected, both remain constant above a certain ‘resting period’ T_r , corresponding to the total activity time (event onset plus refractory period). For $T > T_r$, the neuron fully recovers before the next input arrives.

The empty region left of the minimum input period T_{\min} indicates an absence of 1:1 phase-locking, with distinct implications for the two scenarios: the excitatory node may show other phase-locked modes (e.g., N:M locking) or exhibit *phase slips* where synchrony is interrupted. Inhibitory nodes do not support higher-order locking but do show phase slips and, at high input frequencies, enter sustained inhibition, preventing output events. However, we focus solely on the simplest 1:1 phase-locked mode.

Between the minimum input period and the resting period $T_{\min} < T < T_r$, deviations from the resting onset $\Delta T(\infty)$ arise due to nonlinear effects like after-hyperpolarization and



(a) Excitatory node ($g_{syn} = 0.2$). A small excitatory bump elicits a spike soon after.



(b) Inhibitory node ($g_{syn} = 5$). A strong and long inhibitory synaptic current elicits a delayed rebound spike.

Fig. 2: eDF simulation samples ($\tau_{decay} = 1$). The onset is significantly longer for inhibitory than for excitatory nodes.

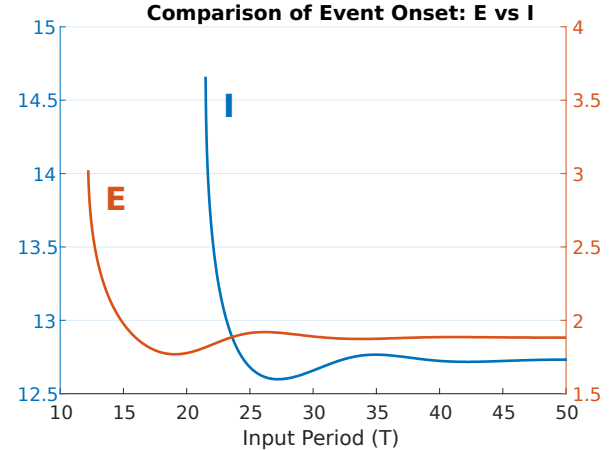
after-depolarization. These effects vary with neuron model and parameter choices and represent periods when the prior event's influence persists into the next input.

The lower panel of Figure 3 shows inhibitory node onset curves for varying synaptic decay constants τ_{decay} and synaptic strengths g_{syn} . Changing g_{syn} only slightly influences T_r , T_{min} , and $\Delta T(\infty)$, mainly affecting the severity of the nonlinear after-spike effects. In contrast, varying τ_{decay} causes clear horizontal and vertical shifts in the onset curves. Consequently, modulation of the synaptic decay time constant offers an effective way to adjust the location and shape of the eDF curve in excitatory nodes.

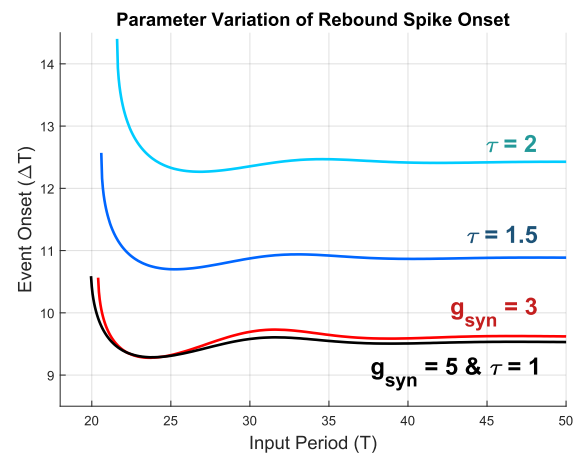
B. Predicting ring network oscillations

A straightforward application of the eDF is in predicting network oscillation existence and period: A ring network of N excitable systems permits a rhythm with period T if the relative phases of its components sum to 1.

$$\sum_{i=1}^N \varphi_i(T) = 1 \quad (5)$$



(a) Absolute phase difference of an inhibitory (I, blue) and excitatory (E, orange) excitable node.



(b) Parameter variation of the inhibitory node: base parameters are $(g_{syn}, \tau_{decay}) = (5, 1)$ and variations show $g_{syn} = 3$ and $\tau_{decay} \in \{1.5, 2\}$

Fig. 3: Absolute onset curves of an excitatory (E) and inhibitory (I) excitable node, and synaptic parameter variations of the inhibitory node.

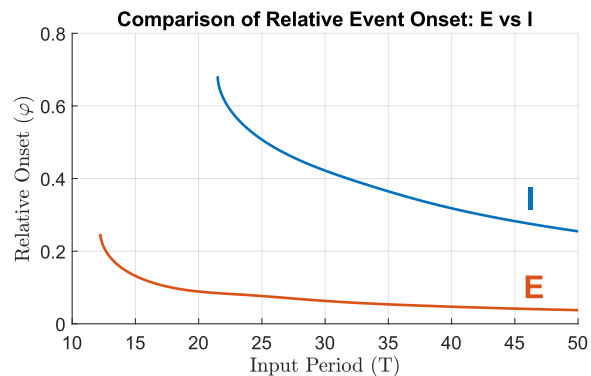


Fig. 4: Event Describing Functions (eDF): relative event onset in function of input period enables graphical prediction of network oscillation period and existence.

where the relative phase of excitable system i at input period T is represented by $\varphi_i(T)$. If we assume a homogeneous ring network, the eDFs in Figure 4 enable simple graphical

predictions of stable oscillation. For instance, we find that the inhibitory eDF curve has an intersection at $\varphi_i(T_N) = 0.5$, which leads to the conclusion that there exists a stable two-node ring network oscillation (at the period of intersection). This inhibitory-inhibitory interconnection corresponds to the half-center oscillator (HCO), which is a fundamental motif in neuroscience and biology, known for its robust rhythmic behavior.

The excitatory eDF, however, does not intersect the value 0.5, and thus two-node ring network oscillations cannot exist, although other stable networks may be found for larger ring sizes.

A similar approach applies to heterogeneous ring networks: summing the individual nodal eDFs and finding the unit intersection (Equation 5) predicts possible oscillation periods. This method enables constructing rings combining inhibitory and excitatory nodes to achieve a desired total period. Moreover, as illustrated in Figure 3b, varying parameters offers a means to control and fine-tune the eDF curves, thereby adjusting network dynamics more precisely.

We can now compare the predictions of the proposed framework to the behavior of a simulated neuronal network. As it turns out, the prediction of oscillation period for an I-I motif (the HCO), is quite accurate, as shown in Table I. The mismatch between the prediction and the realistic oscillation period stems from the modeling mismatch between the Dirac delta impulses and the spiking waveform. Since the spike width somewhat depends on its cause (excitation or rebound) in the HH-model, so does the exact trajectory of the synaptic current. For example, rebound spikes tend to have a slightly longer duration, thus our input impulses, which have a constant width, may underestimate the onset time. Such a negative bias on the eDF could be mitigated by balancing out this effect by increasing the synaptic conductance, or by increasing the effective impulse duration. Because of such underestimation, the prediction may become more inaccurate in the nonlinear regime of small periods.

Ring type	Prediction eDF	Simulation
I-I	25.31	25.43
I-I-I-I	50.93	51.19
E- x10	15.17	15.48

TABLE I: Predicted and simulated network period for various configurations. Inhibitory nodes have $g_{syn} = 5$ and excitatory nodes have $g_{syn} = .2$.

The monotonicity of the event describing function (eDF) implies that there can be only a single intersection point, corresponding to a unique network oscillation solution. This uniqueness is closely related to the stability of the solution: a monotonically increasing or decreasing eDF curve functions as an indicator for local stability. Such relations between monotonicity and stability have been central in the work of Angeli and Sontag [21], [22]. While

this property holds for the Hodgkin-Huxley-type systems considered here, it may not generalize to all excitable or neuronal models.

V. EVENT PHASE RESPONSE CURVES

In the previous section, we developed the event describing function (eDF) as an input-output framework to characterize the frequency-dependent response of excitable systems. Here, we take a complementary perspective and focus on perturbation sensitivity. Specifically, we extend the classical phase response curve (PRC) concept to event-based systems, introducing the event phase response curve (ePRC). This framework captures how periodic synaptic perturbations affect the timing of the periodically forced discrete-event system, providing a relevant insights into its behavior under interaction.

A. Event phase response curves (ePRC)

We propose the event phase response curve (ePRC) as an event-based analogue of the classical PRC for excitable systems. The ePRC quantifies the time shift induced by a periodic synaptic perturbation on a nominal periodic event oscillation of the same period. Periodic perturbations are applied through a synapse, rather than directly perturbing the trajectory, allowing variation of synaptic parameters and providing a biologically realistic description of network interaction.

The classical PRC measures the phase shift between a nominal oscillation and its perturbed (steady-state) counterpart. Analogously, the ePRC of an excitable system is defined with respect to a nominal event-based oscillation (as illustrated in Figure 1b), which requires a nominal periodic input event sequence. The nominal event delay of the system is characterized by its describing function (see Section IV). Perturbations are introduced at phase t_p within each period of the nominal oscillation, producing an additional phase shift beyond the nominal delay. Consequently, the ePRC defines the relationship between the input phase and the resulting output phase shift.

The ePRC framework enables the prediction of interaction dynamics in network oscillations, where the nominal input period of each node corresponds to the overall network period T_N . When T_N is sufficiently large, each input event is isolated, allowing the neuron to return to rest before the next event. In this case, the eDF may be computed from a single nominal event triggered by a single input event. Conversely, when T_N is small and the network dynamics prevent full recovery between events (corresponding to the nonlinear regime of after-spike effects described in Section IV-A), the ePRC must be derived from the complete nominal event oscillation.

The perturbations represent external inputs, for example from sensor nodes acting as proportional feedback elements in a rhythmic control loop [23]. The ePRC therefore captures

how an excitable neuron responds to external stimuli relative to an extrinsic event oscillation.

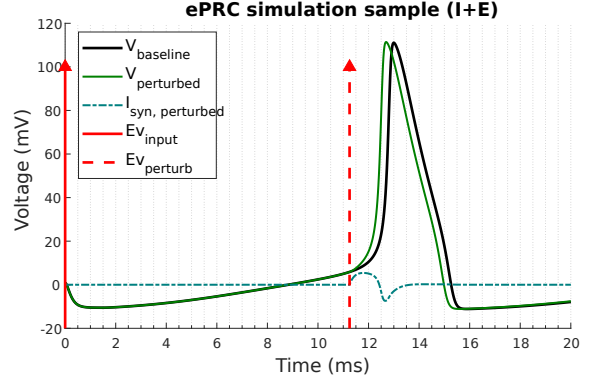
B. Case study: ePRC of a Hodgkin–Huxley neuron

We next apply the ePRC framework to the discrete-event node (introduced in Section III) configured in its rebound-type excitable mode. Perturbations are applied via an excitatory and inhibitory synapses, resulting in the ePRCs illustrated in Figure 5b. Throughout this study, we adopt the standard sign convention where a positive PRC value denotes a phase delay, and define the perturbation time $t_p = 0$ when the perturbation coincides with the nominal input event. The variable t_p is not restricted to positive values; negative t_p correspond to perturbations delivered before the nominal input event, effectively preconditioning the internal states of the neuron.

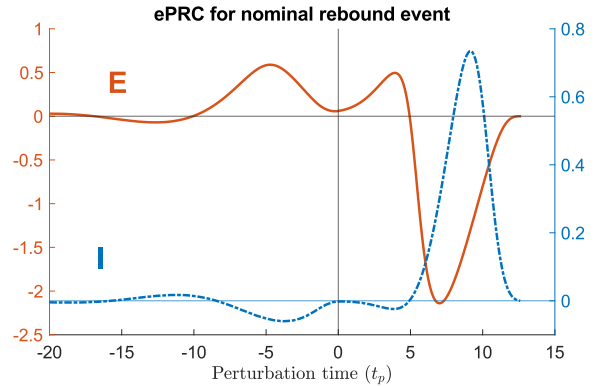
Figure 5a presents the ePRC simulation outcome for the inhibitory synapse perturbed by an excitatory event. The example shows an instance where the perturbation induces a delay in event timing ($\delta(t_p) > 0$). Repeating this simulation over a range of t_p for excitatory and inhibitory perturbations yields the ePRCs in Figure 5b. The excitatory ePRC exhibits three zero crossings (neglecting small values for $t_p < -15$ and including the rightmost zero), indicating potential phase-locking equilibria. The middle equilibrium ($t_p \approx 5$) is unstable due to its negative slope, whereas the far-right equilibrium coincides with the baseline output time and thus later perturbations do not affect the timing at all.

The different regions of the ePRC can be interpreted biophysically: (1) a delayed excitation facilitates recovery from inhibition, advancing the spike; (2) excitation near the onset of baseline inhibition reduces Na-current de-inactivation, slowing recovery and delaying the spike; and (3) an early excitation partially activates the K-current, which also slows recovery from inhibition and delays the spike. The perturbation has negligible influence during most of the network oscillation, which is reasonable since, in many contexts, such inputs merely fine-tune timing (for example, ankle-ground contact in a locomotor gait).

By vertically shifting the ePRC to mimic frequency mismatch between the forcing input and the intrinsic network period, we can explore entrainment properties [24]. A downward shift (lower forcing frequency) introduces a new stable equilibrium near $t_p \approx 0$, removes the in-phase equilibrium, and enlarges the attraction basin of the leftmost equilibrium. Conversely, an upward shift (higher forcing frequency) leaves the rightmost equilibrium as the only stable point. This indicates that inhibitory network oscillations entrain in-phase and robustly when the forcing frequency exceeds the intrinsic network frequency. The effective frequency mismatch is limited by the peak amplitude (near $t_p \approx 7$), since excessive mismatch, and thereby a large vertical shift, can eliminate all zero crossings.



(a) Phase advance caused by an excitatory perturbation. The nominal input event (solid red) elicits a nominal rebound spike (black). The perturbation input (dashed red) causes a change in synaptic current (dashed teal), resulting in an advanced output spike (green).



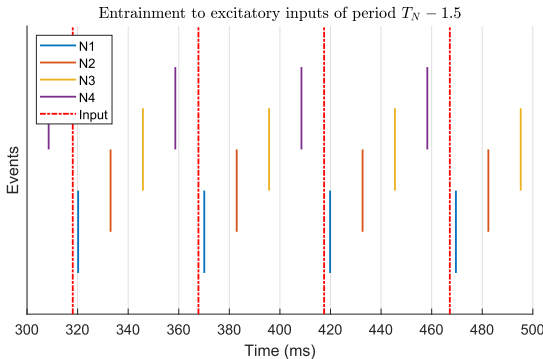
(b) ePRCs for excitatory (orange) and inhibitory (dashed blue) perturbations on separate axes.

Fig. 5: ePRC simulation for a baseline inhibitory rebound spike.

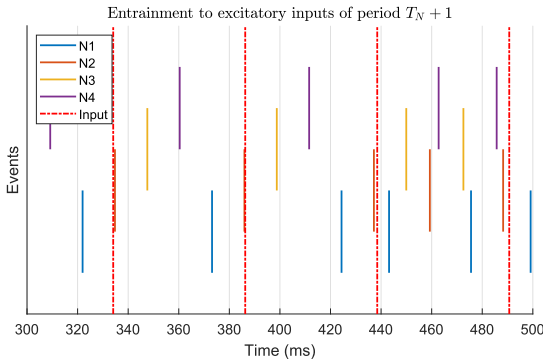
As mentioned in Section V-A, the computation of the ePRC starting from rest assumes a sufficiently long network oscillation period to avoid nonlinear after-spike effects. In Figure 6, a ring of four inhibitory nodes with an intrinsic period $T_N = 51.2$ is driven by excitatory inputs at both higher and lower frequencies. As expected, the network remains phase-locked to the forcing when its period is shortened: the ePRC predicts a stable equilibrium at $\Delta T = -1.5$, corresponding to a lag of $t_p \approx 8.8$. Conversely, when the forcing period is increased, phase-locking is lost.

An analogous result holds for inhibitory perturbations, which produce a mirrored ePRC: entrainment remains stable for lower forcing frequencies, while higher frequencies disrupt synchronization. The same analysis can be repeated for excitatory nodes, leading to a similar set of conclusions based on the qualitative shape of their ePRCs.

Overall, these results indicate that inhibitory neurons entrain robustly to periodic inhibitory inputs at lower or matching frequencies (out of phase) and to excitatory inputs at higher frequencies (in phase). Excitatory neurons can similarly entrain either in or out of phase depending on the forcing frequency, offering practical insights for interaction-based controller design. Within the excitable framework, understanding sensory interactions at the network level thus



(a) Entrainment occurs for raised input frequencies ($\Delta T = -1.5$).



(b) No entrainment occurs for lowered input frequency ($\Delta T = 1$).

Fig. 6: Entrainment simulation validation for ring network of four inhibitory nodes. The intrinsic network period is $T_N = 51.2$. Periodic excitatory perturbations are applied for increased ($T_N + 1$) and decreased ($T_N - 1.5$) period.

reduces to analyzing the response properties of individual nodes. Such an approach offers practical guidance for the design of phase-based controllers.

VI. CONCLUSION

This work has introduced a novel framework extending classical describing function and phase response curve methodologies to excitable neuronal systems. By focusing on event-based input-output characteristics of synapse-neuron nodes, the proposed event describing function (eDF) and event phase response curve (ePRC) provide valuable tools to analyze and predict rhythmic dynamics in excitable networks. The validation through Hodgkin-Huxley neuron simulations illustrates the practical utility of this framework in predicting network oscillations and phase-locking behavior.

Extending the analysis to burst-excitable systems and more complex, realistic CPG architectures remains an important direction for future research. We envision that these developments will facilitate the design and control of biologically inspired rhythmic circuits for robotics and neuromorphic engineering.

REFERENCES

- [1] G. B. Ermentrout and N. Kopell, “Oscillator Death in Systems of Coupled Neural Oscillators,” *SIAM J. Appl. Math.*, vol. 50, pp. 125–146, Feb. 1990.
- [2] A. T. Winfree, *The Geometry of Biological Time*, vol. 12 of *Interdisciplinary Applied Mathematics*. New York, NY: Springer New York, 2001.
- [3] E. Marder and D. Bucher, “Central pattern generators and the control of rhythmic movements,” *Current Biology*, vol. 11, pp. R986–R996, Nov. 2001.
- [4] E. M. Izhikevich, *Dynamical Systems in Neuroscience: The Geometry of Excitability and Bursting*. The MIT Press, July 2006.
- [5] Y. Huo, F. Forni, and R. Sepulchre, “A Winner-Takes-All Mechanism for Event Generation,” Apr. 2025. arXiv:2504.11374 [eess].
- [6] G. Ghirardo, B. Čosić, M. P. Juniper, and J. P. Moeck, “State-space realization of a describing function,” *Nonlinear Dyn*, vol. 82, pp. 9–28, Oct. 2015.
- [7] H. K. Khalil, *Nonlinear systems*. Pearson new international edition, Essex: Pearson Education Limited, third edition ed., 2014.
- [8] T. Wang, “Analyzing Oscillators using Describing Functions,” Sept. 2017. arXiv:1710.02000 [math].
- [9] R. M. Smeal, G. B. Ermentrout, and J. A. White, “Phase-response curves and synchronized neural networks,” *Phil. Trans. R. Soc. B*, vol. 365, pp. 2407–2422, Aug. 2010.
- [10] J. Guckenheimer and P. Holmes, *Nonlinear Oscillations, Dynamical Systems, and Bifurcations of Vector Fields*, vol. 42 of *Applied Mathematical Sciences*. New York, NY: Springer New York, 1983.
- [11] P. Sacre and A. Franci, “Singularly perturbed phase response curves for relaxation oscillators,” in *2016 IEEE 55th Conference on Decision and Control (CDC)*, (Las Vegas, NV, USA), pp. 4680–4685, IEEE, Dec. 2016.
- [12] G. Bordyugov, U. Abraham, A. Granada, P. Rose, K. Imkeller, A. Kramer, and H. Herz, “Tuning the phase of circadian entrainment,” *J. R. Soc. Interface*, vol. 12, p. 20150282, July 2015.
- [13] D. Efimov, P. Sacre, and R. Sepulchre, “Controlling the phase of an oscillator: A phase response curve approach,” in *Proceedings of the 48th IEEE Conference on Decision and Control (CDC) held jointly with 2009 28th Chinese Control Conference*, (Shanghai), pp. 7692–7697, IEEE, Dec. 2009.
- [14] W. Qiao, J. T. Wen, and A. Julius, “Entrainment Control of Phase Dynamics,” *IEEE Trans. Automat. Contr.*, vol. 62, pp. 445–450, Jan. 2017.
- [15] E. M. Izhikevich, “Phase Equations for Relaxation Oscillators,” *SIAM J. Appl. Math.*, vol. 60, pp. 1789–1804, Jan. 2000.
- [16] J. Cui, C. C. Canavier, and R. J. Butera, “Functional Phase Response Curves: A Method for Understanding Synchronization of Adapting Neurons,” *Journal of Neurophysiology*, vol. 102, pp. 387–398, July 2009.
- [17] F. H. Sieling, S. Archila, R. Hooper, C. C. Canavier, and A. A. Prinz, “Phase response theory extended to nonoscillatory network components,” *Phys. Rev. E*, vol. 85, p. 056208, May 2012.
- [18] D. Wilson and J. Moehlis, “Extending Phase Reduction to Excitable Media: Theory and Applications,” *SIAM Rev.*, vol. 57, pp. 201–222, Jan. 2015.
- [19] A. L. Hodgkin and A. F. Huxley, “A quantitative description of membrane current and its application to conduction and excitation in nerve,” *The Journal of Physiology*, vol. 117, pp. 500–544, Aug. 1952. Publisher: Wiley.
- [20] W. Gerstner, ed., *Neuronal dynamics: from single neurons to networks and models of cognition*. S.l.: Cambridge Univ. Press, 2014.
- [21] D. Angeli, J. E. Ferrell, and E. D. Sontag, “Detection of multistability, bifurcations, and hysteresis in a large class of biological positive-feedback systems,” *Proc. Natl. Acad. Sci. U.S.A.*, vol. 101, pp. 1822–1827, Feb. 2004.
- [22] D. Angeli and E. Sontag, “Monotone control systems,” *IEEE Trans. Automat. Contr.*, vol. 48, pp. 1684–1698, Oct. 2003.
- [23] R. Schmetterling, F. Forni, A. Franci, and R. Sepulchre, “Neuromorphic Control of a Pendulum,” *IEEE Control Syst. Lett.*, vol. 8, pp. 1235–1240, 2024.
- [24] D. B. Forger, *Biological clocks, rhythms, and oscillations: the theory of biological timekeeping*. Cambridge, Massachusetts: The MIT Press, 2017.